applied sciences

MDPI

Article

Flexural Strength of Composite Deck Slab with Macro Synthetic Fiber Reinforced Concrete

Dong-Hee Son [1], Baek-Il Bae [2], Moon-Sung Lee [3], Moon-Seok Lee [1] and Chang-Sik Choi [1,*]

[1] Department of Architectural Engineering, Hanyang University, Seoul 04763, Korea; son91com@hanyang.ac.kr (D.-H.S.); leems9076@gmail.com (M.-S.L.)
[2] Department of Digital Architectural and Urban Engineering, Hanyang Cyber University, Seoul 04763, Korea; bibae@hycu.ac.kr
[3] Division of Architecture and Architectural Engineering, Hanyang University, ERICA Campus, Ansan 15588, Korea; moonlee@hanyang.ac.kr
* Correspondence: ccs5530@hanyang.ac.kr

Abstract: In this research, flexural performance was evaluated using macro-synthetic fiber-reinforced concrete (MFRC) in structural deck plates. Material tests were performed to evaluate the mechanical properties of the MFRC, and the flexural strength evaluation was conducted in two experiments, positive and negative moment tests. In the material test results, compressive strength and modulus of elasticity of the MFRC were increased compared with normal concrete. Flexural tensile tests showed that, after achieving maximum strength, the deck plates had sufficient residual strength until fracture. Structural tests showed that flexural strength and cracking load of all specimens increased according to macro synthetic fiber dosage. According to the experimental results, we proposed a flexural strength model of a steel deck plate containing macro synthetic fiber. The model showed greater accuracy than the current standard compared with the experimental results. In addition, since it was confirmed that the MFRC steel decks had greater flexural stiffness until yielding, it will be necessary to quantitatively evaluate the effect of MFRC on the effective flexural stiffness of steel decking in future studies.

Keywords: macro-synthetic fiber; steel deck; flexural performance; flexural strength; deflection

Citation: Son, D.-H.; Bae, B.-I.; Lee, M.-S.; Lee, M.-S.; Choi, C.-S. Flexural Strength of Composite Deck Slab with Macro Synthetic Fiber Reinforced Concrete. *Appl. Sci.* **2021**, *11*, 1662. https://doi.org/10.3390/app11041662

Academic Editor: Jeongsoo Nam
Received: 25 January 2021
Accepted: 8 February 2021
Published: 12 February 2021

1. Introduction

As more buildings are becoming high-rise, composite slab systems using deck plates are being applied to improve constructability, reduce construction time, and address economic feasibility. Deck plates are categorized as either formwork or structural deck plates, depending on the usage. The structural deck plate has advantages that the deck plate itself acts as a formwork when pouring concrete and does not require temporary work such as props. In addition, when a structural deck plate is permanent, it can resist tensile force without reinforcement.

However, in slabs such as steel decking, the reinforcement ratio is low, and a larger area is exposed to air than in other structural members. This can cause wide cracks in a building. Additionally, cracks occur in a slab for various reasons, such as shrinkage and creep. To prevent this, only shrinkage and temperature reinforcement bars are placed on top of the deck plate. However, additional reinforcing bars increase construction time, process, and costs. Moreover, when a structural deck plate is constructed as a continuous span, the wire mesh used as the upper rebar is cold-formed and allows very little elongation. The member will not have sufficient ductility because it has less than the minimum reinforcement ratio. Therefore, one method for preventing upper cracks in a slab and improving the flexural performance of the negative moment region of the deck plate is to apply fiber-reinforced concrete.

Fibers incorporated for crack control are generally reinforced with microfibers, such as steel fiber, glass fiber, and polypropylene; all of these fibers show excellent crack control [1]. Therefore, since an upper reinforcing bar is not required, workability increases, process steps are reduced, and economic efficiency is improved. Structural performance is improved because the tensile strength is increased, and deflection can be reduced by improving effective flexural stiffness. The flexural strength increase reduces the upper tensile reinforcement in the negative moment region. However, if the size of a microfiber crack increases to a macro level, the fiber is pulled out, and the bridge effect decreases, resulting in a rapid decrease in fiber performance [2,3].

Interest in macro fibers with large diameters and long lengths is increasing as they may present a solution to the problems of microfibers. Macro fibers are specified as being at least 0.022 mm in diameter and 38 mm in length; fibers of smaller size are microfibers [4]. A previous study [2,5] showed that concrete containing macro fibers maintained high tensile strain and tensile strength above a certain level, even with large crack widths. Gracez et al. [6] and Nematzadeh et al. [7] reported that when macro-synthetic fiber is incorporated into concrete, the ultimate compressive strain increases with the macro-synthetic fiber dosage. In addition, it is reported that the flexural tensile strength and residual strength increase as the fiber dosage increases.

According to another study [8], introducing macro fiber into reinforced concrete slabs is effective in controlling cracks, reducing deflection, and improving flexural strength. Therefore, in this research, crack patterns and flexural strength were evaluated using macro-synthetic fiber-reinforced concrete (MFRC) in structural steel deck plates. According to the previous research [6], MFRC is effective in improving the flexural strength, and the method of quantitatively evaluating the flexural strength of MFRC without reinforcement using the residual strength improved by macro-synthetic fiber is proposed. In addition, according to previous study [9], when applying steel fiber-reinforced concrete to a structural deck plate, it is possible to simplify the process and improve structural performance by replacing the upper temperature reinforcement. However, when MFRC is applied to a steel deck, the change in the strain of the cross-section and the yield of steel deck have not been considered yet, and the method of quantitatively evaluating the flexural strength is also limited to reinforced concrete slabs [8,10–11]. Therefore, in this study, based on the experimental results, when macro-synthetic fibers are applied to the steel deck, the flexural behavior is analyzed, and, finally, the flexural strength of the MFRC steel deck is evaluated quantitatively. The flexural strength evaluation is conducted in two experiments. First, the flexural strength is evaluated through four-point loading tests for the positive moment under simply supported conditions. Then, the flexural performance of the negative moment region for the continuous span is evaluated through three-point loading tests on inverted specimens.

2. Mechanical Properties of MFRC

2.1. Characteristics of MFRC

To design a steel deck using macro-synthetic fiber, it is necessary to understand the mechanical properties of MFRC. The macro-synthetic fiber used in this study was a synthetic polypropylene hydrophobic fiber that effectively prevents loss of constructability by not reacting with water during mixing [12]. Thus, the friction between fibers and cement matrix can be enhanced by increasing the density of hardened cement paste and, accordingly, decreasing the water-to-cement ratio or adding supplementary cementitious materials [13]. Macro-synthetic fibers have different reinforcing properties depending on shape and size [14]; the twisted and fibrillated bundle shapes used in this study were selected to effectively resist large crack widths, in a ratio of about 9:1. The specifications of the individual fibers used in this study are shown in Table 1 and Figure 1.

Table 1. Fiber specifications [15,16].

Tensile Strength (MPa)	Modulus of Elasticity (GPa)	Length (mm)	Diameter (mm)	Aspect Ratio
54.9	4.7	54	0.34	159

For the concrete mix proportion, the slump was set to 180 mm to secure the workability regardless of the macro-synthetic fiber type. The concrete mix proportions are shown in Table 2. The optimal fiber dosage of the macro-synthetic fiber was determined to be 2.4 kg/m^3, which has the best efficiency according to previous studies [6]. According to a previous study [8], as a result of material test of 0~4.5 kg/m^3 macro-synthetic fiber, the compressive strength decreased at 4.5 kg/m^3, and the increase in flexural tensile strength was similar to that when 2.4 kg/m^3 was incorporated. In addition, as it was confirmed that the workability decreased when 4.5 kg/m^3 was reinforced, the macro synthetic fiber dosage was determined to be 2.4 kg/m^3 in this study. As a result of slump test [17] after mixing concrete, the slump was found to be 180~190 mm, and it is expected that there will be no decrease.

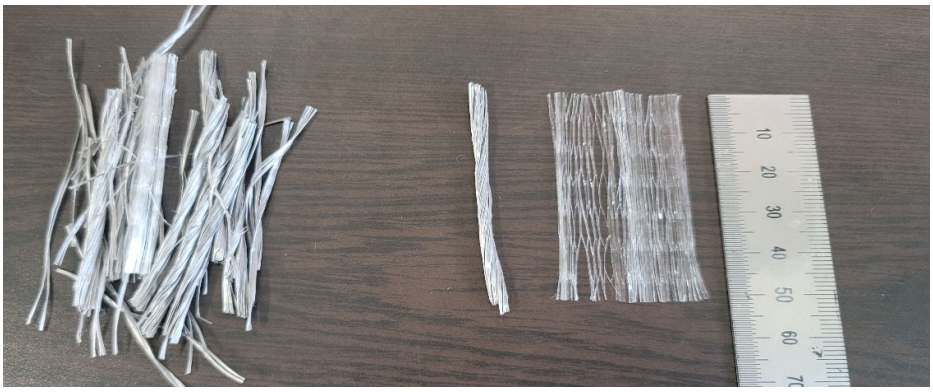

Figure 1. Macro-synthetic fiber.

Table 2. Mix proportions of concrete.

W/C (%)	S/a (%)	Unit Weight (kg/m^3)					
		C	W	S	G	AD	MF
54.9	45.5	365	200.7	854	1022.7	3.29	0
							2.4

W/C: water–cement ratio, S/a: fine aggregate ratio, C: cement, W: water, S: fine aggregate, G: coarse aggregate, AD: admixture, MF: macro-synthetic fiber.

2.2. Compressive Behavior

The concrete compressive test specimens were manufactured with a size of Φ100 × 200 mm according to KS F 2403 [18], and the compressive strength test was performed according to KS F 2405 [19]. For each mix proportion, three specimens were cured for 28 days and tested. The results of the compressive strength tests are shown in Table 3 and Figure 2. The compressive strength of the concrete with 2.4 kg/m^3 of macro-synthetic fiber increased by about 14% compared to normal concrete. The modulus of elasticity was calculated through the slope at the concrete compressive stress corresponding to $0.45f_c'$, as suggested in ACI 318-19 [20,21]. This confirmed that the modulus of elasticity increased as macro-synthetic fibers were incorporated.

Table 3. Concrete compressive test results.

No.	V_f (kg/m³)	f_c' (MPa)	ε_0 (mm/mm)	E_c (MPa)
1	0	34.70	0.00163	38,912
2		34.98	0.00167	35,457
3		35.74	0.00143	41,128
1	2.4	39.35	0.00164	42,408
2		40.94	0.00140	46,054
3		39.89	0.00194	32,934

V_f: macro synthetic fiber dosage, f_c': compressive strength of concrete, ε_0: strain at peak stress, E_c: modulus of elasticity.

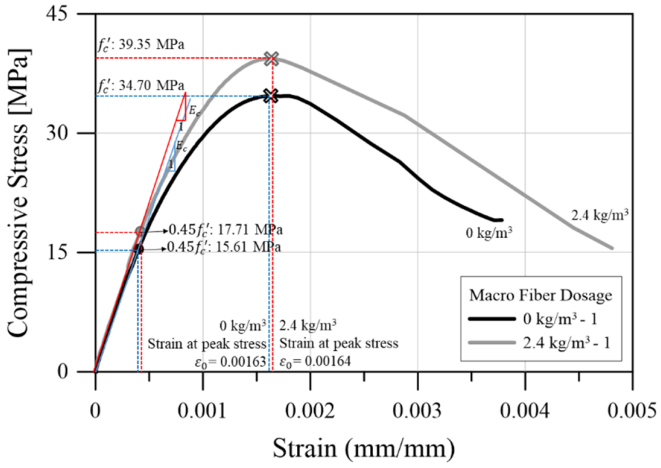

Figure 2. Compressive stress–strain curves.

2.3. Tensile Behavior

According to previous studies [6,7], macro-synthetic fibers are effective in improving the toughness and tensile strength of concrete. Accordingly, in this study, splitting and flexural tensile tests were performed to confirm the tensile strength and flexural toughness of the MFRC according to KS F 2423 [22] and KS F 2408 [23], respectively. The specimens for tensile strength test were made according to KS F 2403 [18]. Splitting and flexural tensile test specimens were manufactured in amounts of 3 and 5, respectively, by mix proportion. The flexural tensile strength test is usually a four-point loading test. However, in fiber-reinforced concrete, it is difficult to measure crack mouth opening displacement (CMOD) after the occurrence of a crack, because the crack likely will occur somewhere other than the center. Therefore, in this study, as suggested in the KS F 2408 appendix, BS EN 14651[24] and fib Model Code 2010 [11], three-point loading tests were performed by creating a central notch.

The results of the flexural tensile strength and splitting tensile strength tests are shown in Table 4. The fib Model Code 2010 [11] defines limit states according to CMOD. A CMOD of 0.5 mm is defined as the serviceability limit state (SLS), and a CMOD of 2.5 mm is defined as the ultimate limit state (ULS). Therefore, the flexural tensile strength was analyzed according to CMOD. Splitting tensile strength and flexural tensile strength did not show much increase with macro-synthetic fiber content. However, after the maximum flexural tensile strength of the MFRC was reached, residual stress was maintained through the tension softening effect, as shown in Figure 3. It is surmised that the macro-synthetic fibers were effective in enhancing the flexural strength.

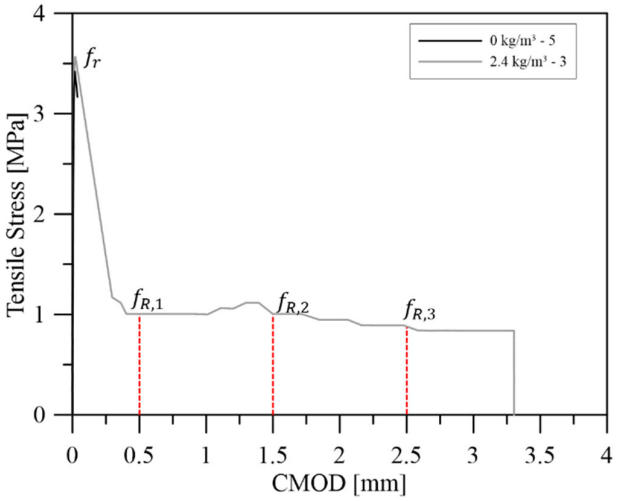

Figure 3. Load–crack mouth opening displacement (CMOD) relationship.

Table 4. Concrete tensile test results.

V_f (kg/m³)	No.	f_{sp} (MPa)	f_r (MPa)	$f_{R,1}$ (MPa)	$f_{R,2}$ (MPa)	$f_{R,3}$ (MPa)	$f_{R,4}$ (MPa)
0	1	3.07	3.62	-	-	-	-
	2	2.78	3.50	-	-	-	-
	3	2.84	3.45	-	-	-	-
	4	-	4.22	-	-	-	-
	5	-	3.42	-	-	-	-
2.4	1	3.09	3.28	1.44	1.39	1.06	-
	2	2.55	3.44	1.45	1.45	1.11	-
	3	3.04	3.57	1.00	0.89	0.89	
	4	-	3.45	-	-	-	-
	5	-	3.11	1.28	1.22	1.11	0.95

V_f: macro synthetic fiber dosage, f_{sp}: splitting tensile stress, f_r: flexural tensile stress, $f_{R,1,2,3,4}$: residual flexural tensile strength corresponding to CMOD = 0.5, 1.5, 2.5, and 3.5 mm, respectively.

3. Experimental Program

3.1. Test Plan and Specimen Design

The steel deck plate used in this study is shown in Figure 4, and its specifications are shown in Table 5. The deck plate was comprised of a hot-dip galvanized steel sheet with a thickness of 0.8 mm, and Y-shaped flanges were added on the top of the deck web to improve the composite behavior of the deck plate and the concrete.

Table 5. Steel deck specifications.

Table 2	Weight (kg/m²)	Section Area (mm²)	Centroid (mm)	Moment of Inertia (mm⁴)
0.8	14.47	1075.2	25.29	915,107

Figure 4. Steel deck plate shape.

The structure of the specimens is shown in Figures 5 and 6. One specimen was manufactured for each test variable. Table 6 details the parameters of the test specimens. When the deck plate was constructed, the deck side did not buckle because the deck plate is continuously arranged or concrete is poured out of the deck by the stopper. Therefore, when fabricating the specimens, concrete was poured to the outside of 50 mm from the side of the deck.

The specimens were classified as positive moment specimens (P- Series) and negative moment specimens (N-series). The positive moment test specimen P-Deck-F0 without macro-synthetic fiber, F2.4 contained 2.4 kg/m^3 of macro-synthetic fiber reinforcement, and the P-deck-F2.4S specimen was welded with a stud at the ends for complete composite action of the concrete and deck plate. According to M.L.Porter [25], the composite slab's failure mode can be categorized three types (shear bond, flexure of under-reinforcement, and over-reinforcement). In this study, in order to check the effect of macro synthetic fiber by failure mode, complete composite behavior was induced through stud welding to prevent shear bond failure.

In the negative moment test specimens, deck plates were installed on both sides of the steel beams, and studs were welded onto the deck for composite behavior of the steel beam and concrete. With the negative moment test specimens, we aimed to evaluate the flexural strength of the continuous end, with the variables of reinforcing macro-synthetic fiber dosage and amount of upper tensile reinforcement. Through this, we tried to confirm how the macro-synthetic fiber affects the flexural performance according to various reinforcement ratios.

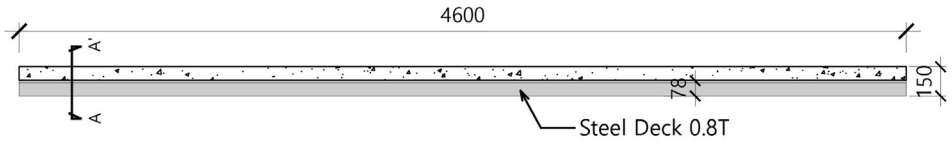

(**a**) Front view (P-Deck-F0, F2.4)

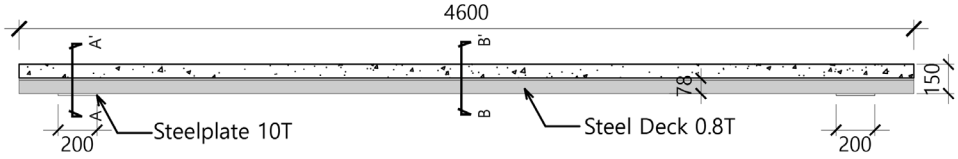

(**b**) Front view (P-Deck-F2.4S)

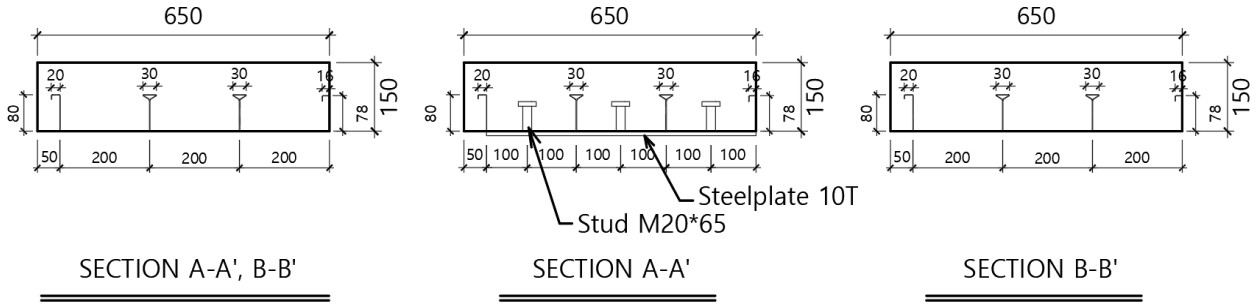

(**c**) Section view (P-Deck-F0, F2.4) (**d**) Section view (P-Deck-F2.4S)

Figure 5. Positive moment test specimen details (unit: mm).

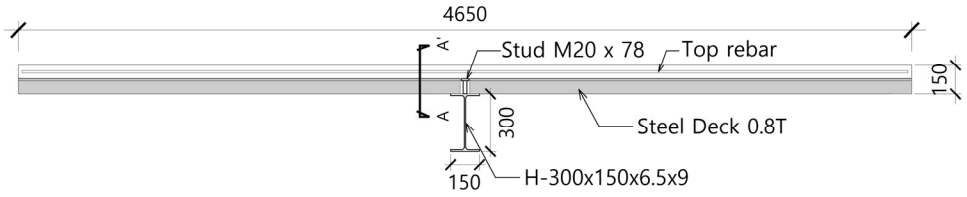

(**a**) Front view

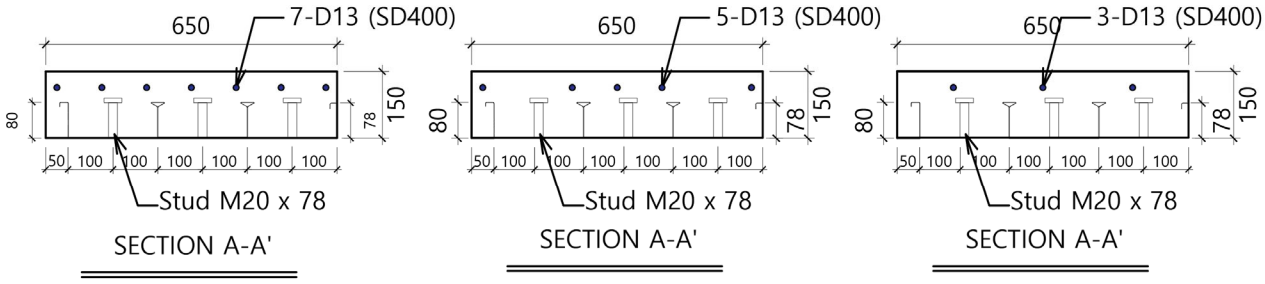

(**b**) Section view (N-Deck-F0, F2.4-R0.91) (**c**) Section view (N-Deck-F0, -R0.65) (**d**) Section view (P-Deck-F2.4S)

Figure 6. Negative moment test specimen details (unit: mm).

Table 6. Specimen details.

ID	Length (mm)	Width (mm)	Thickness (mm)	Shear Span Ratio	$f_{y,deck}$ (MPa)	$A_{s,bot}$ (mm²)	$A_{s,top}$ (mm²)	Macro synthetic fiber (kg/m³)	Remarks
P-Deck-0	4000	650	150	10.8	365	825.6 (Deck)	-	0	-
P-Deck-F2.4								2.4	
P-Deck-F2.4S									Stud 3-M20 (Both ends)
N-Deck-F0-R0.91				16			886.9 (7-D13)	0	-
N-Deck-F2.4-R0.91							886.9 (7-D13)	2.4	
N-Deck-F2.4-R0.65							633.5 (5-D13)		
N-Deck-F2.4-R0.39							380.1 (3-D13)		

$f_{y,deck}$: yield strength of the steel deck, $A_{s,bot}$: deck cross-sectional area, $A_{s,top}$: top rebar cross-sectional area.

The deck plate used in the experiment was SGC 365Y steel grade, as suggested in KS D 3506 [26]. The yield strength was 365 MPa, and the modulus of elasticity was 210,000 MPa. The upper reinforcement of the negative moment test specimen was D13 SD400, and the test was performed according to KS D 0802 [27]. In the rebar test, yield strength was 412.9 MPa and yield strain was 0.0021.

3.2. Test Setup

The test configuration to evaluate the flexural performance of the central region and continuous end region of the steel deck plate with MFRC is shown in Figure 7. In the positive moment test, a four-point loading test was performed. A load cell was installed at each loading point to determine equal loading. In the negative moment test, a deck plate was installed on the H beam to simulate installation in an actual steel structure. The specimen was turned over, and a three-point loading test was performed at the location of the H beam; in this way, the reinforcement placed above the deck plate was simulated to resist the tensile force. The upper and lower flanges were reinforced to prevent local buckling of the H-beam web. Linear variable differential transformers (LVDTs) were installed in the center of the specimen for displacement control [28]. The device used to load the specimen is an actuator.

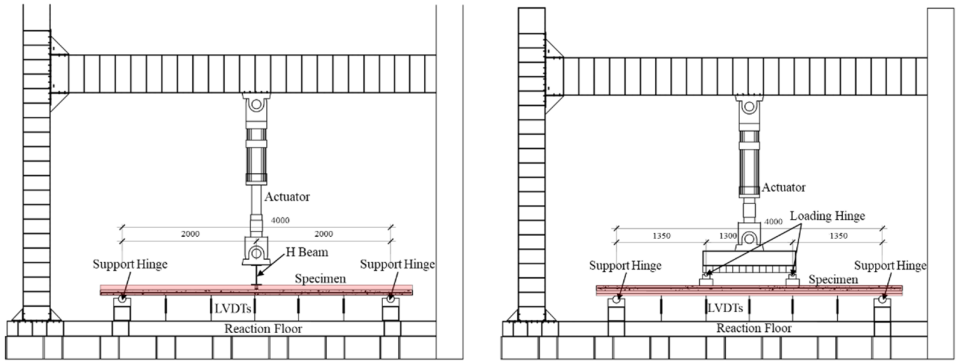

(**a**) Positive moment test (**b**) Negative moment test

Figure 7. Test setup (unit: mm).

4. Test Results

4.1. Crack Propagation and Failure Modes

In the bending tests of the deck plate slabs reinforced with MFRC, all specimens showed flexural failure patterns (Figures 8 and 9). In the P-Deck-F0, an initial flexural crack occurred at a load of about 5kN. Subsequently, as greater load was applied, a crack appeared, indicating shear-bond failure at the location of the deck rib height of 78 mm. This behavior was typical of partial-composite action, which occurs if the horizontal shear-transfer device is not effective enough for the steel deck and concrete to act as a unit without the occurrence of slip [25,29–31]. After that, the deck plate buckled and was fractured by the crushing of concrete.

In the P-Deck-F2.4 specimen, the initial flexural crack occurred later than in P-Deck-F0. In addition, the shear-bond failure pattern occurred in P-Deck-F0, but the crack width and length were small. The spacing of the flexural cracks in P-Deck-F2.4 was shorter than that of P-Deck-F0. This indicates that the macro-synthetic fiber was effective in crack control. After that, local buckling of the deck plate occurred at the loading point as in the P-Deck-F0 specimen, and the experiment ended with the crushing of concrete.

P-Deck-F2.4S was designed to confirm the flexural behavior of the deck plate and concrete in complete composite action. The initial crack in the specimen was not visually significantly different from that of P-Deck-F2.4. Therefore, the exact initial cracking point

was determined as the point at which the strain of the deck plate increased rapidly and the point at which the slope of the load–displacement relationship graph rapidly changed. This confirmed that cracks occurred later than in P-Deck-F2.4, and no shear-bond failure occurred between the deck plate and concrete. This means that a stud was required for complete composite action between the steel deck and concrete. The spacing of the flexural cracks was similar to that of P-Deck-2.4, and fracture occurred after crushing of the upper concrete.

(**a**) P-Deck-0 (left)

(**b**) P-Deck-0 (right)

(**c**) P-Deck-F2.4 (left)

(**d**) P-Deck-F2.4 (right)

(**e**) P-Deck-F2.4S (left)

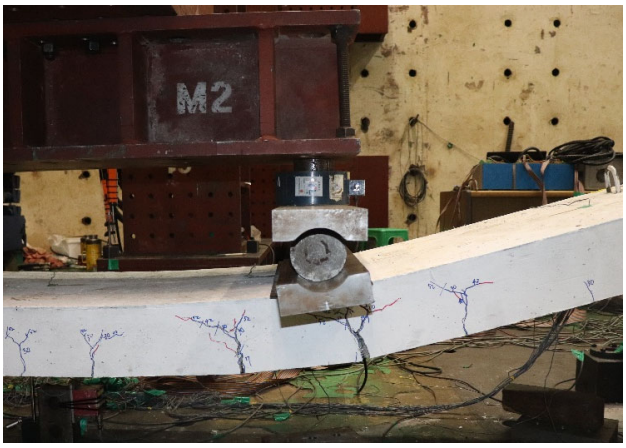

(**f**) P-Deck- F2.4S (right)

Figure 8. Crack and failure patterns (positive moment test specimens).

The N-series specimen tests were performed with a three-point loading test, and flexural failure occurred in all the specimens. The failure patterns of the specimens are shown in Figure 9. The average crack spacing of the N-Deck-F2.4-R0.91 specimen was 18 mm shorter than that of the N-Deck-F0-R0.91 specimen with the same reinforcement ratio.

In the N-Deck-F2.4-R0.65 and N-Deck-F2.4-R0.39 specimens with less reinforcement, flexural failure also occurred. As the reinforcement ratio decreased, the crack gaps widened. In particular, in N-Deck-F2.4-R0.39 with the minimum reinforcement ratio, the crack spacing was quite wide, but the displacement ductile ratio was 13.5, showing a ductile failure pattern.

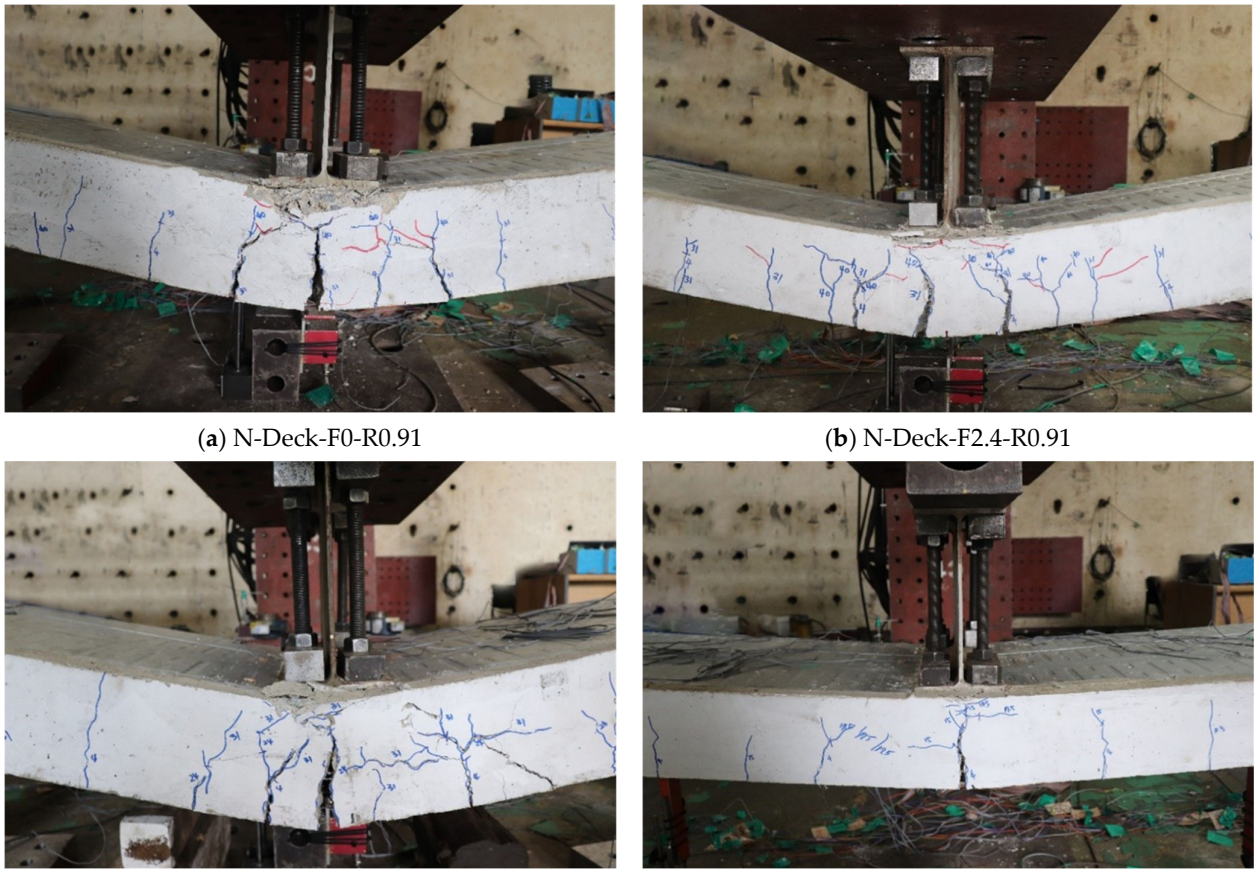

(**a**) N-Deck-F0-R0.91 (**b**) N-Deck-F2.4-R0.91

(**c**) N-Deck-F2.4-R0.65 (**d**) N-Deck-F2.4-R0.39

Figure 9. Crack and failure patterns (negative moment test specimens).

The test results and the load–displacement relationships are shown in Table 7 and Figure 10, respectively. The yield point of each specimen was calculated as the point at which the bottom of the deck plate or tensile reinforcement reached the yield strain. The cracking load was determined based on the first point of decrease in initial stiffness in the load–deflection relationship and the point at which the deformation rate of the deck plate and reinforcement rapidly increased, and the results are shown in Table 8.

The tensile strength of the macro-synthetic fibers was not considered when calculating nominal flexural strength P_n because the calculation assumed complete composite of steel deck and concrete, and the entire section of the deck yielded [20,29]. Similarly, calculating the cracking load f_r did not consider the effect of the macro-synthetic fiber. The calculation and test results were compared considering self-weight, as discussed below.

In the P-Deck-F0 and F2.4 specimens, maximum strength increased with macro-synthetic fiber content. The deflection at maximum load was similar between the two specimens, but the F0 specimen showed a rapidly decreased load after the maximum load. In contrast, the F2.4 specimen slowly decreased in moment resistant capacity after maximum load.

To confirm the initial crack, the graph was enlarged and analyzed (Figure 10bd). The initial cracking load increased as macro-synthetic fibers were incorporated, confirming that macro-synthetic fibers can improve crack strength and increase effective flexural stiffness.

In the negative moment test, in the R0.91 series specimen with a reinforcement ratio of 0.91%, the flexural strength increased as macro-synthetic fibers were incorporated. As the reinforcement ratio decreased, the value of $P_{max,sw}/P_n$ increased. According to ACI 318-19 [20] and ASCE standard specifications [29], the flexural strength conservatively evaluates the actual strength, so the residual strength of MFRC should be considered when calculating flexural strength.

There was no significant difference in the cracking point of the negative moment region due to macro-synthetic fiber dosage. However, when macro-synthetic fiber is mixed, it has greater flexural stiffness at yield. Thus, it is expected that MFRC will have greater effective flexural stiffness, as in the positive moment test.

Table 7. Test results of ultimate flexural load.

ID	Theoretical Value	Test Results						
	P_n (kN)	Δ_y (mm)	P_y (kN)	$P_{max,test}$ (kN)	$P_{max,sw}$ (kN)	$P_{max,sw}/P_n$ (mm)	Δ_{max} (mm)	μ_Δ (mm)
P-Deck-0	66.67	36.52	30.44	49.09	58.26	0.87	204.86	5.61
P-Deck-F2.4		35.54	30.79	51.31	60.48	0.91	204.04	5.74
P-Deck-F2.4S		26.80	26.78	69.82	78.99	1.18	225.16	8.40
N-Deck-F0-R0.91	39.02	32.04	30.39	40.95	50.12	1.28	288.97	9.02
N-Deck-F2.4-R0.91		26.83	30.18	44.23	53.40	1.37	306.46	11.42
N-Deck-F2.4-R0.65	28.52	23.24	21.48	33.8	42.97	1.51	288.34	12.41
N-Deck-F2.4-R0.39	17.50	21.65	12.39	19.09	28.26	1.62	291.35	13.46

P_n: nominal flexural load, P_y, Δ_y: yield load and deflection when bottom deck (rebar) strain reached yield strain, $P_{max,sw}$: modified maximum load considering weight of the specimen, Δ_{max}: displacement at P_{max}, μ_Δ: displacement ductility.

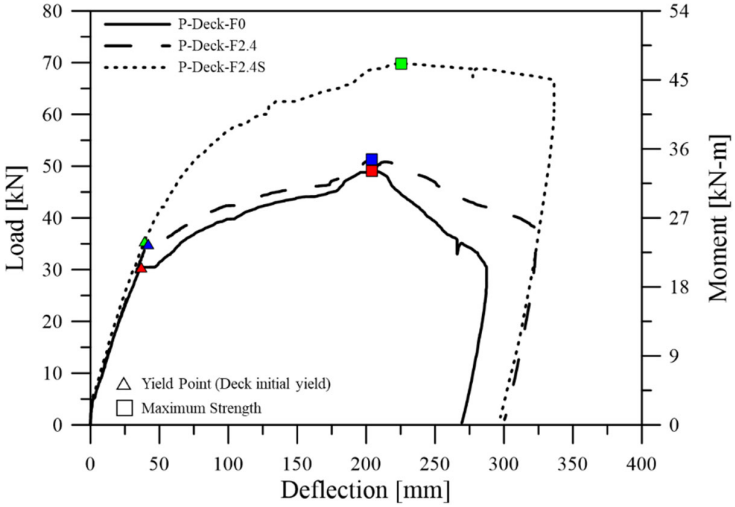

(**a**) Positive moment test—overall behavior

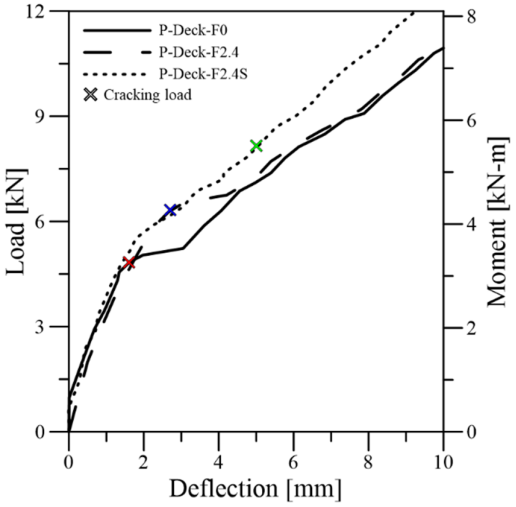

(**b**) Positive moment test—initial behavior

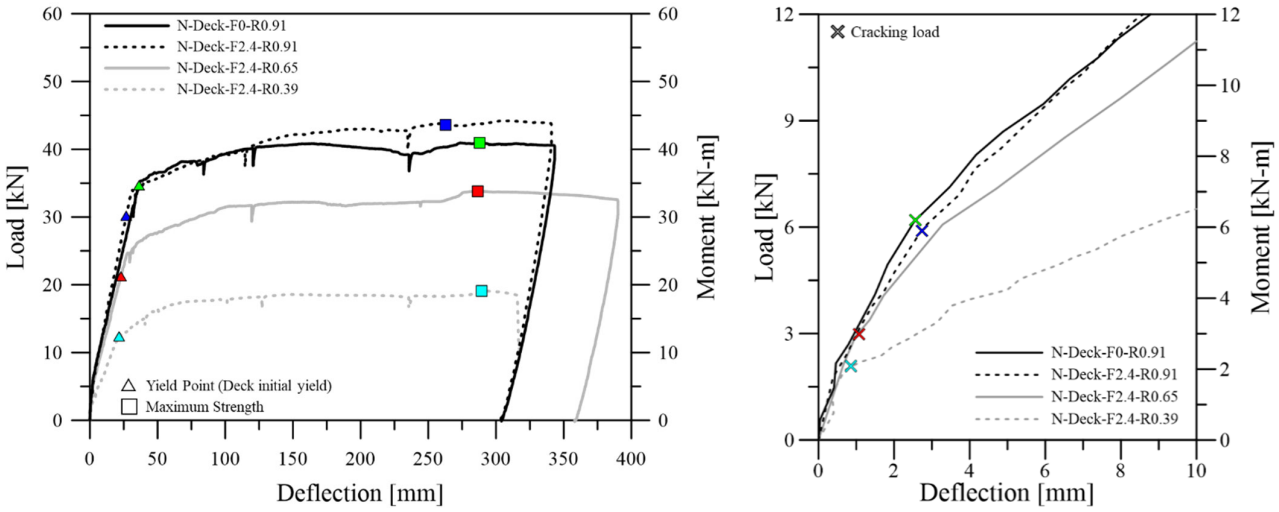

(**c**) Negative moment test—overall behavior (**d**) Negative moment test—initial behavior

Figure 10. Load–displacement relationships.

Table 8. Test results of cracking load.

ID	Theoretical Value $P_{cr,cal}$ (kN)	Test Results			
		$P_{cr,test}$ (kN)	$P_{cr,sw}$ (kN)	$\Delta_{cr,test}$ (mm)	$\frac{P_{cr,sw}}{P_{cr,cal}}$
P-Deck-0	12.17	4.85	14.02	1.85	1.15
P-Deck-F2.4		6.26	15.43	2.37	1.27
P-Deck-F2.4S		7.98	17.15	5.01	1.41
N-Deck-F0-R0.91	8.21	6.07	15.24	2.47	1.86
N-Deck-F2.4-R0.91		5.85	15.02	2.71	1.83
N-Deck-F2.4-R0.65		3.47	12.64	1.37	1.54
N-Deck-F2.4-R0.39		2.26	11.43	1.03	1.39

$P_{cr,cal}$: cracking load, $P_{cr,test}$: cracking load at initial flexural crack, $P_{cr,sw}$: cracking load considering self-weight of specimen, $\Delta_{cr,test}$: displacement at initial flexural crack.

4.2. Strain Distribution of a Section

To evaluate the flexural strength of the deck plate reinforced with MFRC in the positive moment region, it was necessary to assess the strain distribution and determine whether the deck yielded over the entire area. For this, the strain distribution at the center of the section was confirmed and is shown in Figure 11. The strain gauge was attached to the web in the center of the specimen. Each gauge was attached to the bottom surface of the specimen, the rib of the deck, the upper part of the deck, and the concrete compression fiber.

The neutral axis depth of P-Deck-F2.4 was larger than that of P-Deck-F0, and the strain at the bottom of the deck was smaller than that of the F0 specimen. This is because MFRC partially resists tensile force according to the amount of macro-synthetic fiber incorporated. In the P-Deck F2.4S specimen, the strain of the steel deck bottom was much greater than that of the other two specimens. This is because the MFRC and steel deck plate were completely composited by studs. Since most of the deck cross-sectional area yielded, it can be assumed that the tensile force of the deck plate acted in the centroid when the flexural strength was calculated.

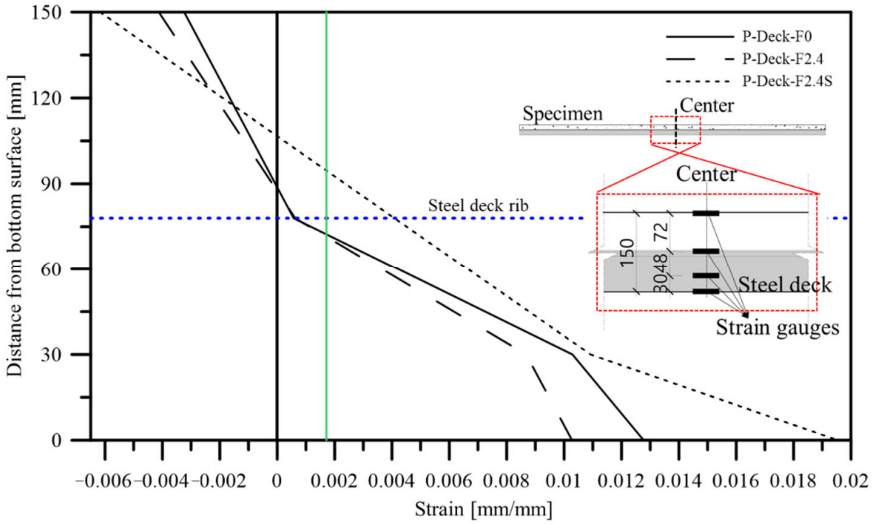

Figure 11. Strain distribution at the center of specimens (unit: mm).

When a load was applied to the negative moment region of the steel deck, it did not significantly affect the flexural strength because the deck plate resisted the compressive force. Therefore, the upper tensile reinforcements were considered only when calculating the flexural strength. The load–strain relationship is shown in Figure 12 to confirm whether the rebar yielded at the point of maximum strength.

The upper tensile reinforcement of all specimens yielded, and the N-Deck-F2.4-R0.39 with minimum reinforcement ratio yielded at the point of maximum strength.

As a result of comparing the R0.91 series specimens at the same reinforcement ratio, as the F2.4 specimen approached the ultimate strength, it showed less tensile strain compared to that at the same load. This is because the MFRC partially resisted the tensile force of the rebar.

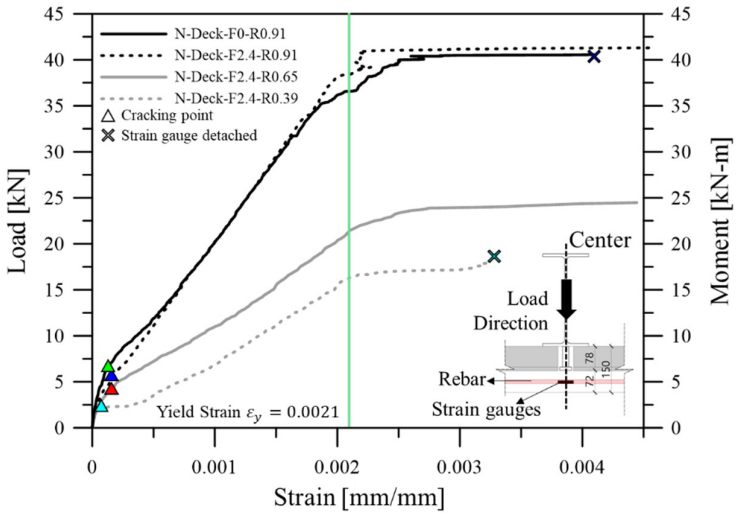

Figure 12. Load–strain relationship (negative moment test specimens; unit: mm).

5. Ultimate Flexural Strength of the MFRC Steel Deck

According to the previous test results, when MFRC is applied to a steel deck plate, the positive moment and the negative moment should be calculated. Here, the flexural strength model of the MFRC was calculated using the flexural strength of steel fiber-

reinforced concrete as suggested in ACI 544.4R-88 [10]. To calculate flexural strength, the flexural tensile stress–strain relationship of concrete should be derived. This can be calculated from the load–CMOD relationship as Equations (1) and (2) [32]:

$$f_t = \frac{3PL}{2bh^2} \tag{1}$$

$$\varepsilon = \frac{f_t}{E_c} + \frac{w}{l_c} \tag{2}$$

here, f_t is flexural tensile strength, P is load, L is length of specimen, b is width of test specimen, h is height of specimen, ε is tensile strain, E_c is modulus of elasticity, w is crack width, and l_c is 2/3h.

As a flexural tensile strength test, the maximum tensile strain of concrete was about 0.03, which was greater than that at the bottom of the deck at the point of maximum strength. Therefore, residual stress could be applied to the region subjected to tensile force. In fib Model Code 2010 [11], the residual stress in the ultimate limit state is defined as CMOD = 2.5 mm; when applying the rigid plastic model, the ultimate residual strength f_{Ftu} can be calculated as in Equation (3):

$$f_{Ftu} = \frac{f_{R,3}}{3} \tag{3}$$

Strain and stress distribution for the calculation of flexural strength is shown in Figure 13. When calculating the flexural strength of the steel deck plate containing macro-synthetic fiber, the depth of the concrete-equivalent stress block can be calculated according to the force equilibrium, as shown in Equation (4):

$$C_c = T_c + T_{deck} \tag{4}$$

here, C_c is the compression force of the MFRC, T_c is the tension force of the MFRC, and T_{deck} is the tension force of the steel deck.

After calculating the depth of the concrete equivalent stress block, the flexural strength can be calculated by Equation (5):

$$M_{n,mfrc} = T_{deck}\left(d - \frac{a}{2}\right) + T_c\left(\frac{H + c - a}{2}\right) \tag{5}$$

here, H is the thickness of the slab, c is the depth of the neutral axis, d is the effective depth of the section, a is the depth of the equivalent rectangular stress block, and $T_c = A_{ct}f_{Ftu} = (H - c)bf_{Ftu}$

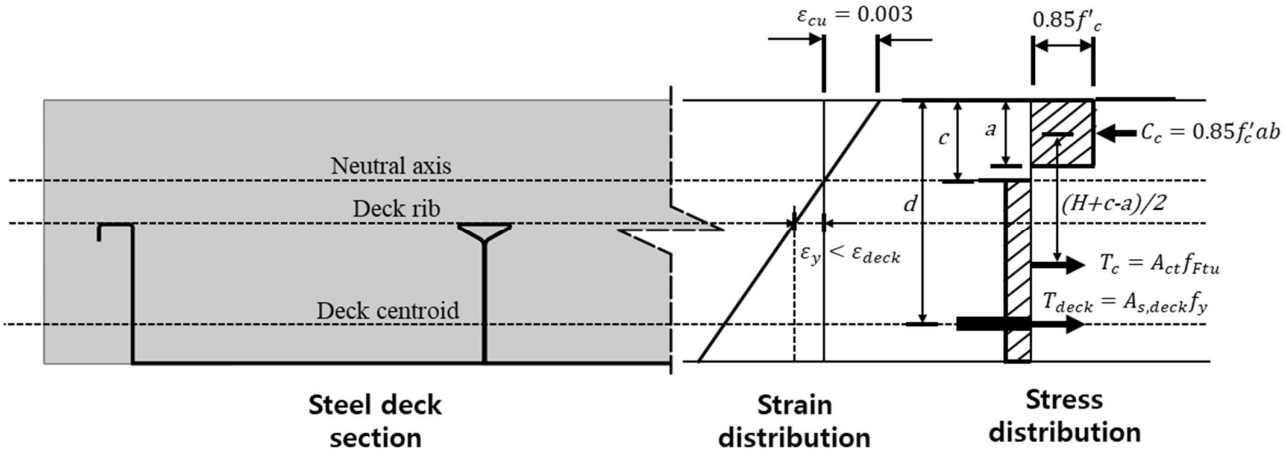

Figure 13. Strain and stress distributions (positive moment).

When calculating the negative moment of a steel deck plate with macro-synthetic fiber, the upper strain was not large, so the flexural strength was calculated without considering the effect of the steel deck in this simple design process. The flexural strength was calculated in the same way as for the steel deck, using Equations (6) and (7):

$$C_c = T_c + T_{rebar} \tag{6}$$

$$M_{n,mfrc} = T_{rebar}\left(d - \frac{a}{2}\right) + T_c\left(\frac{d + c - a}{2}\right) \tag{7}$$

However, unlike when obtaining the positive moment, the concrete did not bear the load in the part beyond the upper tensile reinforcing bar. Therefore, the area where the concrete bore the tensile force was set to b (d-c), and the strain and stress distributions for this are shown in Figure 14.

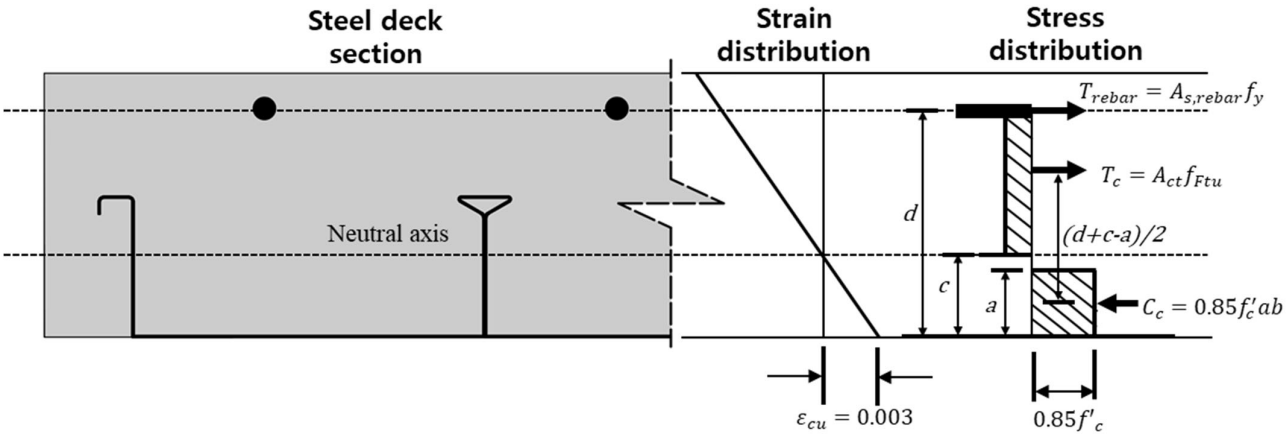

Figure 14. Strain and stress distributions (negative moment).

Based on the previously proposed flexural strength evaluation model, the experimental results and the proposed model were compared, and the results are shown in Table 9. Since the stress and strain distributions acting on the cross section were calculated by assuming the complete composite of the positive moment specimen, only P-Deck-F2.4S was considered, and the negative moment specimen was compared with the proposed model for all specimens. All the specimens predicted flexural strength more accurately when considering the flexural contribution of the macro-synthetic fiber. In addition, more accurate results are expected if the compressive force received by the deck is considered when calculating the flexural strength through precise cross-sectional analysis.

Table 9. Comparison of ultimate flexural strength between the standard [20,29] and the model proposed here.

	$M_{n,mfrc}$ (kN-m)	$P_{n,mfrc}$ (kN)	$P_{max,sw}$ (kN)	$P_{max,sw}/P_n$	$P_{max,sw}/P_{n,mfrc}$
P-Deck-F2.4S	47.43	70.26	78.99	1.18	1.12
N-Deck-F2.4-R0.91	46.03	46.03	53.40	1.37	1.16
N-Deck-F2.4-R0.65	34.04	34.04	42.97	1.51	1.26
N-Deck-F2.4-R0.39	21.55	21.55	28.26	1.62	1.31

$M_{n,mfrc}$: flexural strength calculated by the proposed model, $P_{n,mfrc}$: load of converting flexural strength with concentrated load $(2M_{n,mfrc}/a)$, a: distance between support and loading point, P_n: nominal flexural load, $P_{max,sw}$: modified maximum load considering weight of the specimen.

6. Conclusions

The aim of this study was to evaluate the flexural strength of a steel deck plate system reinforced with MFRC. To accomplish this, we conducted a four-point loading test for the positive moment and a three-point loading test for the negative moment. In the positive moment test, macro synthetic fiber dosage and existence of studs were the main variables. Macro synthetic fiber dosage and reinforcement ratio were the main variables in the negative moment test. From these experiments under limited conditions, the following conclusions were obtained.

(1) In the uniaxial compressive strength test of concrete reinforced with macro-synthetic fiber, compressive strength and modulus of elasticity increased. Furthermore, the strength decreased more gradually after achieving the maximum compressive strength of the MFRC. In the flexural and splitting tensile strength tests, unlike other research results [6,7] in which the tensile strength increased, there was little change in both parameters. It is judged that when the macro-synthetic fiber dosage is 2.4 kg/m^3, the fiber dosage is small; thus, the maximum tensile strength cannot be increased. However, after achieving the maximum strength, the specimens had sufficient residual strength until fracture.

(2) The flexural strength and cracking load of all specimens increased according to macro synthetic fiber dosage. The increase in flexural strength was more pronounced in the negative moment region than in the positive moment region. In addition, since it was confirmed that the MFRC steel deck had greater flexural stiffness until yielding, it will be necessary to quantitatively evaluate the effect of MFRC on the effective flexural stiffness of steel decking in future studies.

(3) According to the experimental results, we proposed a flexural strength model of a steel deck plate containing macro synthetic fiber. This model showed greater accuracy than the current standard when comparing the experimental results. However, due to the simple design process described here, the equation proposed does not consider the compressive force contributed by the steel deck. If the compressive force of the steel deck was considered in the precise analysis, it would be possible to predict flexural strength more accurately.

(4) In future studies, the effect of macro-synthetic fiber on flexural strength could be predicted more accurately by performing flexural strength evaluation using various macro-synthetic fibers. Furthermore, when fiber-reinforced concrete is applied to a new slab system, the contribution of the fiber to the flexural strength could be examined.

Author Contributions: Original draft preparation and editing, D.-H.S.; performing tests and investigations, D.-H.S., Moon-Seok Lee; analyzing the results and reviewing the article; B.-I.B., Moon-Sung Lee; supervision and review writing, C.-S.C. All authors have read and agreed to the published version of the manuscript.

Funding: This research was supported by the Basic Science Research Program through the National Research Foundation of Korea (NRF) funded by the Ministry of Education (NRF-2018R1A2B6009483 and NRF-2020R1A4A1019074).

Institutional Review Board Statement: Not applicable.

Informed Consent Statement: Not applicable.

Data Availability Statement: Data is contained within the article or supplementary material.

Conflicts of Interest: The authors declare no conflict of interest.

References

1. Kim, M.-H.; Kim, J.-H.; Kim, Y.-R.; Kim, Y.-D. An Experimental Study on the Mechanical Properties of HPFRCCS Reinforced with the Micro and Macro Fibers. *J. Korea Concr. Inst.* **2005**, *17*, 263–271.
2. Chun, B.; Yoo, D.Y. Hybrid Effect of Macro and Micro Steel Fibers on the Pullout and Tensile Behaviors of Ultra-High-Performance Concrete. *Compos. Part B Eng.* **2019**, *162*, 344–360.
3. Şahin, Y.; Köksal, F. The influences of matrix and steel fibre tensile strengths on the fracture energy of high-strength concrete. *Constr. Build. Mater.* **2011**, *25*, 1801–1806, doi:10.1016/j.conbuildmat.2010.11.084.
4. Lawler, J.S.; Zampini, D.; Shah, S.P. Microfiber and Macrofiber Hybrid Fiber-Reinforced Concrete. *J. Mater. Civ. Eng.* **2005**, *17*, 595–604.
5. Ryu, H.-S.; Kim, D.-M.; Shin, S.-H.; Ryu, I.-H.; Joe, J.-M. Evaluation on Mechanical Properties of Organic of Fiber Reinforced Concrete Using Macro Forta Fiber. *J. Korea Inst. Build. Constr.* **2017**, *17*, 321–329.
6. Oliari, G.; Estela, M.I.K.; Alastair, M.; Mahbube, S.; Kazem, G. Self-Compacting Concrete Reinforced with Twisted-Bundle Macro-Synthetic Fiber. *Appl. Sci.* **2019**, *9*, 2543.
7. Nematzadeh, M.; Hasan-Nattaj, F. Compressive Stress-Strain Model for High-Strength Concrete Reinforced with Forta-Ferro and Steel Fibers. *J. Mater. Civ. Eng.* **2017**, *29*, 04017152.
8. Lee, M.S.; Chung, J.H.; Son, D.H.; Choi, C.S. Flexural Strength Evaluation of Reinforced Concrete Slabs with Macro Synthetic Fibers. *J. Archit. Inst. Korea* **2020**, *36*, 241–248. (In Korean)
9. Hong, G.H. Structural Performance of Steel Fiber Reinforced Concrete Continuous Slab without Reinforcement. *J. Archit. Inst. Korea Struct. Constr.* **2015**, *31*, 11–18.
10. ACI Committee. *ACI 544.4R-88, Guide to Design with Fiber-Reinforced Concrete*; ACI Committee: Farmington Hill, MI, USA, 1988.
11. Taerwe, L.; Matthys, S. *Fib Model Code for Concrete Structures 2010*; Ernst & Sohn, Wiley: Berlin, Germany, 2013.
12. FORTA-FERRO Company. *Macro Synthetic Fiber Technical Report*; FORTA Concrete Fiber Company: Grove City, PA, USA, 2018.
13. Smirnova, O.; Kharitonov, A.; Belentsov, Y. Influence of polyolefin fibers on the strength and deformability properties of road pavement concrete. *J. Traffic Transp. Eng.* **2019**, *6*, 407–417.
14. Daneshfar, M.; Hassani, A.; Aliha, M.R.M.; Berto, F. Evaluating Mechanical Properties of Macro-Synthetic Fiber-Reinforced Concrete with Various Types and Contents. *Strength Mater.* **2017**, *49*, 618–626, doi:10.1007/s11223-017-9907-z.
15. Nematzadeh, M.; Fallah-Valukolaee, S. Erosion resistance of high-strength concrete containing forta-ferro fibers against sulfuric acid attack with an optimum design. *Constr. Build. Mater.* **2017**, *154*, 675–686.
16. Hasan-Nattaj, F.; Nematzadeh, M. The effect of forta-ferro and steel fibers on mechanical properties of high-strength concrete with and without silica fume and nano-silica. *Constr. Build. Mater.* **2017**, *137*, 557–572, doi:10.1016/j.conbuildmat.2017.01.078.
17. Korean Agency for Technology and Standards. *KS B 2402. Standard Test Method for Concrete Slump*; Korean Agency for Technology and Standards: Seoul, Korea, 2017; pp. 1–14.
18. Korean Agency for Technology and Standards. *KS F 2403. Standard Test Method for Making and Curing Concrete Specimens*; Korean Agency for Technology and Standards: Seoul, Korea, 2014; pp. 1–14.
19. Korean Agency for Technology and Standards. *KS F 2405. Standard Test Method for Compressive Strength of Concrete*; Korean Agency for Technology and Standards: Seoul, Korea, 2014; pp. 1–16.
20. ACI Committee. *ACI 318-19. Building Code Requirement for Structural Concrete and Commentary*; ACI Committee: Farmington Hill, MI, USA, 2019.
21. Pauw, A. Static Modulus of Elasticity of Concrete as Affected by Density. *ACI J. Proc.* **2016**, *57*, 679–688, doi:10.14359/8040.
22. Korean Agency for Technology and Standards. *KS F 2423. Method of Test for Splitting Tensile Strength of Concrete*; Korean Agency for Technology and Standards: Seoul, Korea, 2016; pp. 1–12.
23. Korean Agency for Technology and Standards. *KS F 2408. Method of Test for Flexural Strength of Concrete*; Korean Agency for Technology and Standards: Seoul, Korea, 2016; pp. 1–16.
24. BSI. *EN, BS. 14651. Test Method for Metallic Fibre Concrete-Measuring the Flexural Tensile Strength (Limit of Proportionally (LOP), Residual)*; BSI: London, UK, 2007; pp. 1–20.
25. Porter, M.L.; Ekberg, C.E. Design Recommendations for Steel Deck Floor Slabs. *J. Struct. Div.-ASCE* **1976**, *102*, 2121–2136.
26. Korean Agency for Technology and Standards. *KS D 3506. Hot-Dip Zinc-Coated Steel Sheets and Coil*; Korean Agency for Technology and Standards: Seoul, Korea, 2018; pp. 1–60.
27. Korean Agency for Technology and Standards. *KS B 0802. Method of Tensile Test for Metallic Materials*; Korean Agency for Technology and Standards: Seoul, Korea, 2013; pp. 1–7.
28. Chung, J.H. Flexural and Shear Behavior of Donut Type Voided Slabs. Ph.D. Thesis, Hanyang University, Seoul, Korea, 2015.
29. ASCE. *Standard for the Structural Design of Composite Slabs and Standard Practice for Construction and Inspection of Composite Slabs*; ANSI/ASCE 2-84; American Society of Civil Engineers: New York, NY, USA, 1994.
30. Easterling, W.S.; Young, C.S. Strength of Composite Slabs. *J. Struct. Eng.-ASCE* **1992**, *118*, 2370–2389.
31. Lamport, W.B.; Porter, M.L. Deflection Predictions for Concrete Slabs Reinforced with Steel Decking. *ACI Struct. J.* **1990**, *87*, 564–570.
32. Kim, K.C.; Yang, I.H.; Joh, C.B. Material Properties and Structural Characteristics on Flexure of Steel Fiber-Reinforced Ultra-High-Performance Concrete. *J. Korea Concr. Inst.* **2016**, *28*, 177–185, doi:10.4334/jkci.2016.28.2.17.